Monatshefte für Chemie 138, 389–401 (2007)
DOI 10.1007/s00706-007-0624-3
Printed in The Netherlands

Monatshefte für Chemie
Chemical Monthly

Cerium(III/IV) and Cerium(IV)–Titanium(IV) Citric Complexes Prepared in Ethylene Glycol Medium

M. Getsova[1], **D. Todorovsky**[1,*], **V. Enchev**[2], and **I. Wawer**[3]

[1] Faculty of Chemistry, University of Sofia, 1, Sofia, Bulgaria
[2] Institute of Organic Chemistry, Bulgarian Academy of Science, Sofia, Bulgaria
[3] Faculty of Pharmacy, The Medical University of Warsaw, Warsaw, Poland

Received August 16, 2006; accepted (revised) November 15, 2006; published online April 12, 2007

Summary. Cerium(III/IV) and Ce(IV)–Ti(IV) citric complexes were synthesized in ethylene glycol medium under conditions similar to those of the polymerized complex method (PCM). Solution phase ^{1}H, ^{13}C NMR, solid state ^{13}C CP MAS NMR and IR spectroscopy, and X-ray powder diffractometry were used to characterize the composition and structure of the synthesized products. Thermal decomposition of the isolated complexes was studied and a scheme of the processes taking place is proposed. Complexes of Ce(III) can be prepared at low temperature (40°C), only. In the presence of Ti(IV) ions, the oxidation takes place even at this temperature. A mixed-metal nature of the Ce(IV)–Ti(IV) complexes is established. The comparison between their composition and the one of analogous lanthanide(III)–Ti(IV) citrates contributes to the elucidation of the complexation process mechanism in the case of the PCM application. The increased charge of the complexation agent in the Ce^{4+}–Ti^{4+} complex (in comparison with Ln^{3+}–Ti^{4+} citrates) is "compensated" by the increase of the relative number of the ligands with deprotonated OH group.

Keywords. Cerium; Metal complexes; NMR spectroscopy; Thermochemistry; Titanium.

Introduction

The polymerized complex method (PCM), a version of the sol–gel technology, approves itself to be an appropriate technique for preparation of multicomponent, phase-homogeneous materials with a good crystalline structure reached at relatively low temperatures. The $Ln_2Ti_2O_7$ (Ln = Y, La, Nd), effective ferroelectrics (Ln = La, Nd) or ionic conductors (Ln = Y) were also produced following this method [1, 2].

In a number of papers [3–7] we reported some data concerning the mechanism of the main processes (complexation, esterification/polyesterification and thermal decomposition) involved in the PCM application. The study was performed on the systems Ln^{3+}–Ti^{4+}–citric acid–ethylene glycol (Ln = Y, La) but the results obtained could be of significance for the elucidation of the processes in similar citric acid–ethylene glycol containing systems.

However, it is rather difficult to look deeper inside in the mechanism of the processes by studying of the real systems obtained by the PCM. The great excess of acid and ethylene glycol in the solutions or in the polyester resins makes systems rather complicated and hinders a detailed investigation. That is why we started with the complexes isolation followed by studying of their composition, some spectral characteristics, and thermal decomposition.

One of the main peculiarities of the complexation process in systems like the above mentioned is the deprotonation of the citric acid alcoholic group taking place at uncommonly low *pH* value in *Ln*(III)–Ti(IV)- [1, 2], Ba–Ti- [8], and Pb–Ti- [9] ethylene glycol-citric systems. The deprotonation of the

* Corresponding author. E-mail: nhdt@wmail.chem.uni-sofia.bg

OH-groups was recently observed in Ti^{4+}–citric acid aqueous systems but at higher *pH*-value [10–12]. The important role of the esterification on the *Ln*–Ti complexes composition, particularly, on the relative content of the ligands with deprotonated OH group was shown in a previous work [5]. The nature of the lanthanide(III) ions influences the composition of the complexes but this influence is revealed indirectly, namely through their efficiency as esterification catalysts [5]. In the present work the effect of the oxidation state of the lanthanide on the complex composition and, particularly, on the degree of OH deprotonation of the ligands is studied in order to confirm or to reject the hypothesis proposed in Ref. [5] concerning the processes responsible for the complexes composition determination and their interaction.

From another point of view the interest in the citric systems and particularly in Ti-citrates considerably increased recently, due mainly to the extended application of Ti in ceramic materials, alloys, and composites in medical technologies [10–12].

Following the main goal of the present work – elucidation of the chemistry of the processes involved in PCM, Ce-, Ti-, and Ce–Ti-complexes were synthesized under conditions as close as possible to the ones of the PCM, including the mole ratio of the components in the initial solution. For preparation of $Ln_2Ti_2O_7$ the mole ratio Ln^{3+}:Ti^{4+}:citric acid:ethylene glycol = 1:1:10:40 has been used [1, 2]. The same ratio was used by us for the Ce–Ti complex synthesis. The molar ratio in the cases of Ce^{3+}- and of Ti^{4+}-complexes preparation was adjusted taking into account the electrical charge of the complexing agents and keeping constant the amounts of the acid and ethylene glycol related to the unity electrical charge. The complexes obtained after heating between 40 and 120°C were isolated and studied.

Results and Discussion

Composition and Structure of Isolated Products

The complexes elemental composition, the content of H_2O (determined thermogravimetrically), the residues after ignition of the complexes up to 1000°C (as percent from the initial mass), and the relative content of ethylene glycol bonded either as adduct or ester are summarized in Table 1. The latter data (derived from ^{1}H NMR spectra) are available only for the complexes viewing complete dissolving in D_2O. By comparison of the intensities of the shifts at 3.8 and 4.2 ppm in ^{1}H spectra the presence and relative amount of doubly esterified $HOCH_2CH_2OH$ are determined. It seems that Ti^{4+} acts as a rather strong esterification catalyst causing such an effect. As can be seen (Table 1) the Ti-complex **4** contains doubly esterified ethylene glycol, bridging two citric ligands and forming species like $[(HOCH_2CH_2–Cit)–CH_2CH_2–(Cit–CH_2CH_2OH)]^{4-}$ (Table 2), where Cit=$CH_2COO–C(O)COO–CH_2COO$.

The yield of the complexes (Table 1) is calculated on the base of the mass of the metals introduced in the starting solution as a ratio between the real mass of the obtained product and the mass expected according to the proposed formulae (Table 2). It depends mainly on the temperature of synthesis and is limited by the solubility of the prepared complexes in the water-acetone mixture used for their isolation. The variations are within the limits of less than 4% of the values shown in Table 1. The composition of the isolated products varies by 2–3% of the averaged values (Table 1) from case to case due to the variation of the degree of the ligand esterification and the content of ethylene glycol, bonded as adduct.

The Ce(III) oxidation state was found by EPR analysis in the product obtained by heating of the initial Ce^{3+}–citric acid–ethylene glycol solution up to 40°C. No EPR signals were recorded in the products obtained by heating of the same solution at 100°C and of analogous solutions of Ce^{4+} at 40 and 100°C. The lack of EPR signals cannot be taken as final evidence for Ce(IV) presence. If the isolated complexes are of a binuclear nature (which is quite probable) no EPR signals will be recorded even if the cerium is present as Ce(III). However, a detailed study of the Ce^{3+}-containing system behavior [13] confirmed that Ce^{4+}-complexes are formed at a heating above ~85°C when either $(NH_4)_2Ce(NO_3)_6$ or $Ce(NO_3)_3$ are used as sources of cerium. This fact is briefly commented bellow.

These results, along with the IR and ^{13}C NMR data allow the composition of the complexes to be described by the formulae given in Table 2.

The presence of hydration water in all separated complexes is evidenced by a broad absorption in the IR spectra with a maximum at ~3400 cm^{-1}. Free and bonded (in adducts) non-dissociated OH groups of the citric ligands also contribute to the 3400–3200 cm^{-1} band intensity. The signal at 4.52 ppm in ^{1}H NMR spec-

Table 1. Composition of the studied complexes (experimentally found values, in brackets – calculated according to the formula proposed in Table 2)

Sample symbol[a]	Ce-source	Temperature of synthesis °C	%						
			H	C	N	Ce	Ti	H_2O	Residue[b]
1	$Ce(NO_3)_3 \cdot 6H_2O$	40	3.38	22.06		30.84		13.1	35.3
			(3.35)	(22.11)		(31.45)		(12.1)	(38.6)
2	$Ce(NO_3)_3 \cdot 6H_2O$	100	3.53	24.01		28.57		11.7	33.7
			(3.30)	(24.18)		(27.66)		(10.7)	(34.0)
3	$(NH_4)_2Ce(NO_3)_3$	100	3.60	24.74	2.01	25.46		10.6	27.7
			(3.70)	(24.66)	(1.51)	(25.24)		(9.7)	(31.0)
4	–	120	5.21	34.44			6.73	9.2	11.9
			(5.60)	(35.62)			(6.07)	(9.1)	(10.1)
5	$Ce(NO_3)_3 \cdot 6H_2O$	100	3.93	27.36		16.00	5.50	11.1	27.0
			(3.96)	(28.27)		(15.13)	(5.17)	(11.1)	(27.2)
6	$(NH_4)_2Ce(NO_3)_3$	100	4.88	30.20	2.09	12.25	4.00	8.2	20.5
			(4.66)	(29.86)	(1.96)	(12.27)	(4.19)	(8.2)	(22.1)

Sample symbol[a]	Mole ratio according to NMR data			Shift at 91 ppm in ^{13}C spectra	Yield of the compound %[d]
	$HO(CH_2)_2OH/L$[c]	$HO(CH_2)_2/L$[c]	$(CH_2)_2/L$[c]		
1	(0.08)	(0.33)	(0)	no	64 ± 3
2	(0.07)	(0.33)	(0)	no	75 ± 4
3	(0.06)	(0.29)	(0)	no	82 ± 4
4	0.90 (0.87)	0.84 (0.83)	0.46 (0.39)	yes	85 ± 3
5	(0.04)	(1.0)	(0)	yes	81 ± 5
6	0.26 (0.27)	0.98 (1.00)	(0)	yes	89 ± 4

[a] See Table 2
[b] After ignition to 1000°C, CeO_2 or/and TiO_2 are accepted as final products
[c] L – citric ligands
[d] Result from 3 batches

Table 2. Proposed formula of studied complexes

Sample symbol	Proposed formula*
1	$Ce^{3+}(H\mathit{Cit}H^{2-})_{0.2}(H\mathit{Cit}^{3-})_{0.6}[H\mathit{Cit}(CH_2)_2OH^{2-}]_{0.4} \cdot 0.1HO(CH_2)_2OH \cdot 3H_2O$
2	$Ce^{4+}(H\mathit{Cit}^{3-})[H\mathit{Cit}(CH_2)_2OH^{2-}]_{0.5} \cdot 0.1HO(CH_2)_2OH \cdot 3H_2O$
3	$(NH_4^+)_{0.6}Ce^{4+}(H\mathit{Cit}^{3-})_{1.2}[H\mathit{Cit}(CH_2)_2OH^{2-}]_{0.5} \cdot 0.1HO(CH_2)_2OH \cdot 3H_2O$
4	$Ti[H\mathit{Cit}(CH_2)_2OH^{2-}]_{0.3}[H\mathit{Cit}(CH_2)_2OH \cdot (CH_2)_2 \cdot H\mathit{Cit}^{3-}]_{0.6}$ $[\mathit{Cit}(CH_2CH_2OH)_2{}^{2-}]_{0.2}[(\mathit{Cit}CH_2CH_2OH)_2(CH_2)_2{}^{4-}]_{0.3} \cdot 2HO(CH_2)_2OH \cdot 4H_2O$
5	$Ce^{4+}Ti^{4+}[H\mathit{Cit}(CH_2)_2OH^{2-}]_{0.1}[\mathit{Cit}(CH_2)_2OH^{3-})_{2.6} \cdot 0.1HO(CH_2)_2OH \cdot 5.7H_2O$
6	$(NH_4^+)_{1.6}Ce^{4+}Ti^{4+}[H\mathit{Cit}(CH_2)_2OH^{2-}]_{0.3}[\mathit{Cit}(CH_2)_2OH^{3-}]_3 \cdot HO(CH_2)_2OH \cdot 5.2H_2O$

* $H\mathit{Cit} = CH_2COO–C(OH)COO–CH_2COO$; $\mathit{Cit} = CH_2COO–C(O)COO–CH_2COO$

tra of the solutions, obtained by dissolving of the complexes in $CDCl_3$, also indicates the presence of H_2O.

The presence of ethylene glycol bonded as adduct is proved by the band at 1044 cm^{-1} in the IR spectra [4] (Fig. 1) and by the presence of resonances at 65.7 ppm and at 3.65 ppm in ^{13}C and ^{1}H NMR spectra [3], respectively and is confirmed by the temperature of its release (above 230°C, boiling point of pure ethylene glycol is 196–198°C).

The ^{13}C signals at 67.3 and 60.4 ppm (Fig. 2) as well as the ^{1}H signals at 3.8 and 4.2 ppm (Fig. 3) are due to methylene carbon proton/hydroxyl proton in esterificated ethylene glycol, *e.g.* HO–$\underline{CH_2}$- and –O–$\underline{CH_2}$- [3]. The esterificated citric ligands exhibit an IR band at 1722 cm^{-1} ($\nu_{(C=O)}$, Fig. 1). As it is shown in Ref. [4], this band is strongly overlapped by the adduct C=O band. The $\nu_{(C-O)}$ of the ester (1198 cm^{-1}) and that of adduct

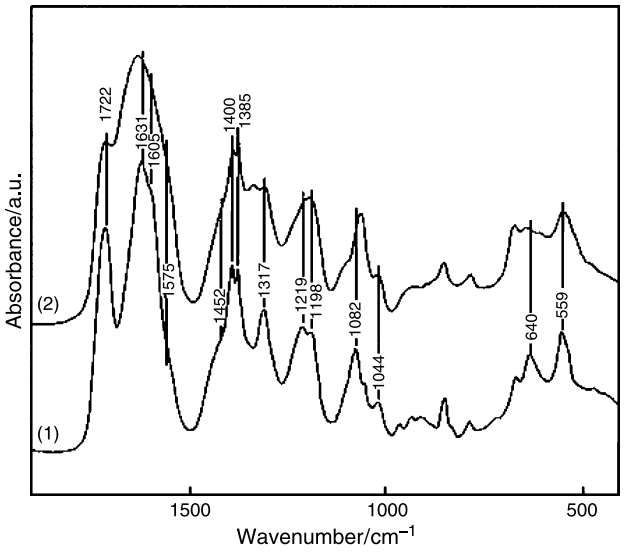

Fig. 1. IR spectra of **6** (1) and **5** (2); for meaning of symbols see Tables 1 and 2

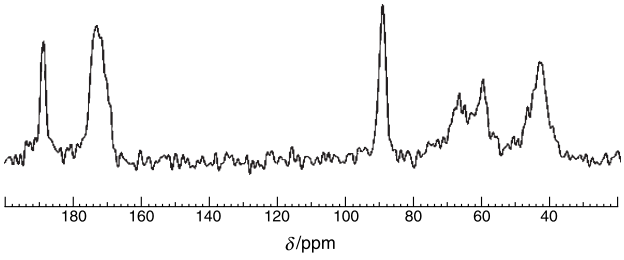

Fig. 2. Solid state ^{13}C NMR spectrum of **6** (see Table 2)

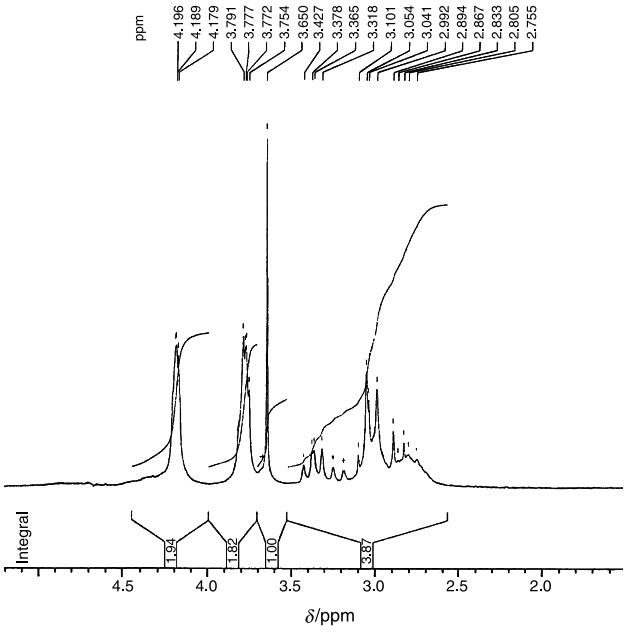

Fig. 3. ^{1}H NMR spectrum of **6** (D_2O-solution) (see Table 2)

(1219 cm^{-1}) [4] are well distinguished (Fig. 1). The ^{13}C NMR signals in the citric acid spectrum at 174.5, 176.1, and 179.0 ppm (Table 3) are caused by the carbonyl carbons in COOH groups of citric acid molecules linked by the hydrogen bonds [14, 15]. Most of these signals do not exist in the spectra of the solid complexes; thus, it has to be accepted that there are no COOH groups in the studied complexes composition. The formulae given in Table 2 are in agreement with such an inference.

The complexation is proved by the characteristic vibration of COO^- groups, corresponding to the antisymmetric and symmetric stretching vibrations near 1600 and 1400 cm^{-1} in the IR spectra. The absorption maxima at 640 and 559 cm^{-1} were assigned to the $\nu^{as}_{(Ti-O)}$ and $\nu^{s}_{(Ti-O)}$ (Fig. 1).

Cerium(III) and Cerium(IV) Complexes

The Ce(III) complex (described as **1** by the formula listed in Table 2) most probably represents a mixture of Ce – complexes differing by the degree of deprotonation and/or esterification of COOH – groups.

Table 3. ^{13}C CPMAS NMR chemical shifts (δ/ppm, ref. *TMS*) of citric acid and citric complexes

Sample symbol[a]	δ CH_2 of $HO(CH_2)_2OH$	Citric acid						
		CH_2	C–OH	C–O	2 × C=O, C=O			
Citric acid hydrate	–	43.6	72.3		174.5, 176.1, 179.0			
4	60.6–66.2	42.2–45.0	74.3	88.0–92.0	170.2	179.2	182.3	185.6
6	60.4–67.3	43.8	–	90.0	172.0, 173.5	–	–	189.0
7[b]	60.4–66.0	43.4	74.0–76.1	88.4	170.6	175.5	180.0	185.7

[a] See Tables 1 and 2

[b] $LaTi[HCit(CH_2)_2OH(CH_2)_2HCit^{3-}]_{0.2}[HCit(CH_2)_2OH(CH_2)_2Cit^{4-}]_{0.2}$
$[Cit(CH_2)_2OH^{3-}]_{1.2}[(CitCH_2CH_2OH)_2(CH_2)_2{}^{4-}]_{0.5} \cdot 0.2HO(CH_2)_2OH \cdot 6H_2O$, for the symbols' meaning see Table 2

Multiplying the formula shown in Table 2 by 5 and accounting for the most common coordination number of the cerium, the following composition could be supposed: $\{3[Ce(HCit)\cdot 2H_2O]\cdot[(HCitCH_2CH_2OH)$–$Ce$–$HCitCH_2CH_2OH$–$Ce$–$HCitH)\cdot 0.5HO(CH_2)_2OH\cdot 4H_2O]\}\cdot 5H_2O$, where $HCit = CH_2COO$–$C(OH)COO$–CH_2COO (*i.e.* citric acid with all of the COOH-groups deprotonated) and H*Cit*H is citric acid with deprotonated and one protonated carboxylic group. Some experimental observations support the above idea. At least two maxima appear in the IR spectrum region just bellow 1600 cm^{-1}, namely at 1593 and 1570 cm^{-1} (Fig. 4.1). The position of the stronger one (1593 cm^{-1}) is quite close to that in the sodium citrate spectrum (1591 cm^{-1}) [16] and is probably due to the stretching vibration of ionized but uncoordinated COO^- groups. The band shifted to the lower frequency side (1570 cm^{-1}) may be due [17] to COO^- groups involved in bridging between the Ce(III) centers in the supposed dinuclear complex. An octahedral coordination with a tetragonal distortion of Ce^{3+} nuclei in the complex follows from the EPR data: $g_1 = 0.90$, $g_2 = 2.45$. The cerium coordination spheres have to be partially completed by water molecules. The latter is confirmed from the thermogravimetric analysis data, showing that approximately 2/3 of the water separates at higher temperature (125–150°C) indicating its coordination to the cerium. As far as the ethylene glycol is bonded by a hydrogen bond to O atom of the C=O group of some of the ligands [4], one could not exclude the possibility for the coordination sphere of Ce^{3+} in Ce(III) citrate **1** to be completed by donor group(s) of the ligands belonging to the other complex.

The Ce complexes **2** and **3** prepared at 100°C have practically the same composition in spite of the oxidation state of the cerium ions added to the initial

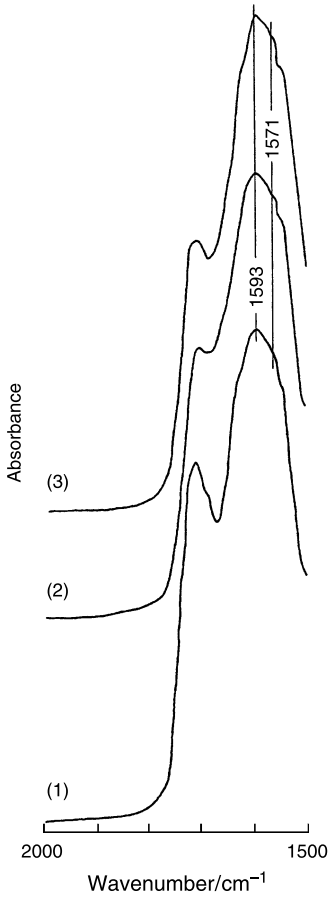

Fig. 4. IR spectra of **1** (1), **2** (2), **6** (3) (see Table 2)

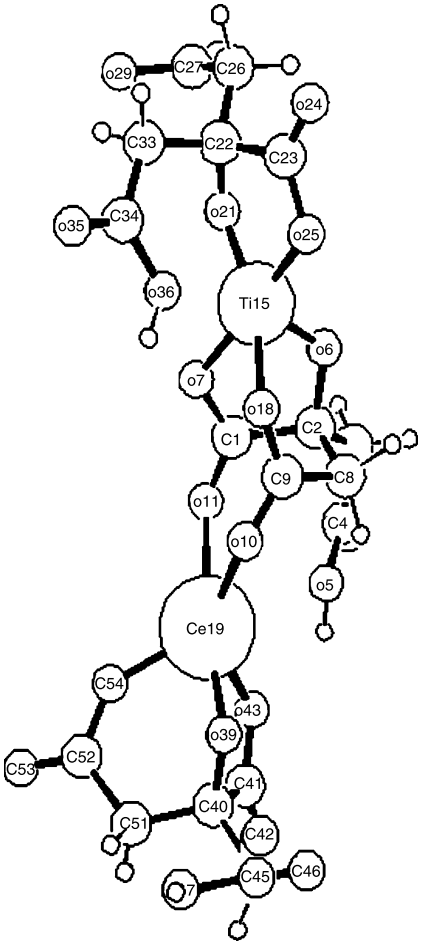

Fig. 5. *Ab initio* calculated structure of $NH_4CeTi[Cit(CH_2)_2OH]_3$. In fact, ethylene glycol remains are connected to oxygen atoms O36, O5, and O46 (see Table 2). For simplicity in the quantum-chemical calculations the ethylene glycol fragments were replaced by hydrogen atoms

solution (Tables 1 and 2). The oxidation of Ce^{3+} is due to HNO_3 (produced by the complexation of the $Ce(NO_3)_3$ with the citric acid) and nitrogen oxide(s) resulted in its thermal decomposition at elevated temperatures.

The difference between the complexes **2** and **3** is caused by the presence of NH_4^+ incorporated in the isolated substances (Table 1) when $(NH_4)_2Ce(NO_3)_6$ is used as Ce^{4+} source. Multiplying the formula given in Table 2 by 2 the NH_4^+-free Ce(IV) complex **2** could be represented as a dinuclear complex $Ce_2(HCit)_2[HCit(CH_2)_2OH] \cdot 0.2HO(CH_2)_2OH \cdot 6H_2O$. The elemental composition of the complex **3** can be satisfactorily described as a mixture of the above shown complex and $(NH_4)_3HCit$, *i.e.* $Ce_2(HCit)_2[HCit(CH_2)_2OH] \cdot 0.2HO(CH_2)_2OH \cdot 6H_2O + 0.4(NH_4)_3HCit$. The latter can be formed in solution along with the Ce-complexes and will be desalted by the added acetone due to its insolubility in acetone. Formation of a similar ammonium citrate is proven by X-ray diffractometry in the course of Ce–Ti-complexes preparation (see next paragraph). The individual Ti(IV) citrate(IV) has been already described in Ref. [6].

Mixed Ce(IV)–Ti(IV) Complexes

The Ce(IV)–Ti(IV) citrates **5** and **6** contain ligands with deprotonated alcoholic group, as indicated by the shift of the resonance signal of the citric acid (*CA*) alcoholic carbon from 72.3 to 89.9 ppm in ^{13}C NMR spectra (Fig. 2, Table 3) [1–3, 18]. A new peak arising at 189.0 ppm (lacking in the acid spectrum) could be assigned to the carbon in the central COO^- group coordinated to the metal ions [18, 19]. Considering the characteristic formation of five-member chelated ring when both OH (being protonated or deprotonated) and COO^- groups (attached to the central carbon atom of the citric ligand) coordinate to the metal ion [20], it is reasonable to be supposed that such a type of coordination takes place as well in the studied Ce(IV)–Ti(IV) compounds **5** and **6**. The simultaneous existence of the signals near 90 and 186–189 ppm is also found in the analogous Ti(IV) and La(III)–Ti(IV) citric complexes [21]. In contrast to the lanthanum–titanium complex, where the central COO^- group of the citric ligands are coordinated at various distances to metal ions, in the Ce(IV)–Ti(IV) citric complex **6** all of the ligands are

Table 4. Selected *ab initio* calculated distances in the Ce–Ti citric complex

	Distances/Å		Distances/Å		Distances/Å
Ti–O25	1.889	C23–O25	1.351	C23–O24	1.216
Ti–O21	1.815	C22–O21	1.437		
Ti–O6	1.852	C13–O6	1.439		
Ti–O18	2.117	C9–O18	1.284	C9–O10	1.277
Ti–O7	2.083	C1–O7	1.273	C1–O11	1.269
Ce–O43	2.206	C41–O43	1.352	C41–O42	1.219
Ce–O39	2.071	C40–O39	1.443		
Ce–O54	2.083	C52–O54	1.364	C52–O55	1.218
Ce–O10	2.410	C9–O10	1.277	C9–O18	1.284
Ce–O11	2.385	C1–O11	1.269	C1–O7	1.273

Table 5. Composition of Ce(IV)-, Ti(IV)-, Ce(IV)–Ti(IV)-, and La(III)–Ti(IV) citrates

Complex[a]	L^b	Z^b	$(CH_2)_2OH/L^b$	$(CH_2)_2/L^b$	$D_{est}{}^c$	L^-/L^b
3[d]	1.5	2.67	0.33	0	0.33	0
4	2.3	1.74	0.83	0.39	1.61	0.35
6[e]	3.0	2.67	1.00	0	1.00	1.00
7[f]	3.0	2.33	0.87	0.30	1.47	0.80

[a] See Table 2
[b] L, mol of ligands; L^-, mol of ligands with a deprotonated OH group; Z, average charge of the ligands; $R = (CH_2)_2$
[c] Esterification degree, $D_{est} = [(CH_2)_2OH + 2(CH_2)_2]/L$
[d] After deducing the ligands relevant to the NH_4^+-ions present
[e] After deducing the ligands relevant to the $(NH_4)_2(HCitROH)$ present
[f] See Table 3

coordinated to metal(IV) ions in the same manner. Indeed, in the solid state ^{13}C NMR spectrum of **6** only one signal exists in the range of carbon of the central COO^- group. The wide and intensive peak at 173 ppm (Fig. 2, Table 3) is caused by the overlapping of the signals of terminal esterified and ionized COOH groups [17, 18]. All of the citric complexes prepared by us under conditions of PCM [3, 5–7, 21] consist of ligands with esterified central carboxylic group, while in the case of **6** such type of ligand does not exist. In the spectrum of the latter complex there is no signal near 176–179 ppm (Fig. 2, Table 3) that could be assigned to central esterified COOH.

Ab initio calculations were performed for the $NH_4\{CeTi[Cit(CH_2)_2OH]_3 \cdot HO(CH_2)_2OH \cdot 5.2H_2O\}$ which is the main part of the product described as **6** in Table 2 (as will be shown below in this paragraph). The molecular structure calculated is shown in Fig. 5. The most important distances in the complex are given in Table 4.

The Ti–O6, Ti–O21, and Ti–O25 distances (1.852–1.889 Å) are typical for the individual Ti-citric complexes (1.852–1.879 Å) reported by *Kefalas et al.* [11] from XRD data. The Ce–O39, Ce–O43, and Ce–O54 distances are longer in comparison with the respective Ti–O ones because of the greater ion radius of Ce(IV). Two carboxylate groups from the central citric acid are bridging the metal ions (Fig. 5). The calculated Ti–O18, and Ti–O7 distances are 2.117 and 2.028 Å. They are in agreement with the experimental X-ray data (2.036–2.055 Å) for the Ti-citric complexes [11]. The respective Ce–O10 (2.410 Å) and Ce–O11 (2.385 Å) distances are again longer than the Ti–O ones.

The $\nu^{as}{}_{(COO^-)}$ bands in the IR spectrum of the NH_4–Ce–Ti citrate **6** at 1631 and ~1605 cm^{-1} (Fig. 1) are shifted to higher frequencies as compared to those of sodium citrate (1591 cm^{-1}). This implies that the COO^- groups coordinate to the central

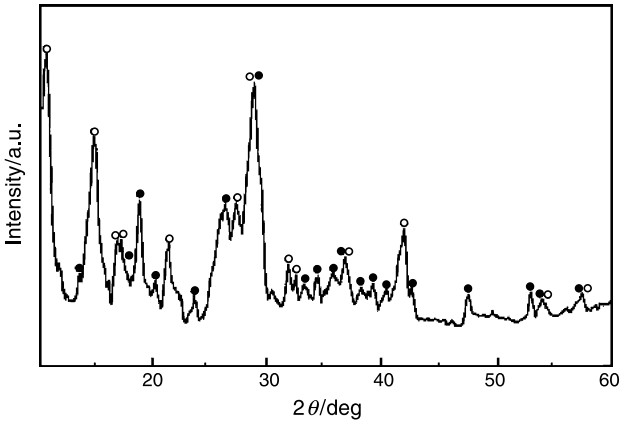

Fig. 6. X-Ray diffractogram of **6** (see Table 2): • – $(NH_4)_2[HCit(CH_2)_2ROH)$, ○ – $NH_4CeTi[Cit(CH_2)_2OH] \cdot HO(CH_2)_2OH \cdot 5.2H_2O$

Table 6. Interplanar distances ($d/10^{-10}$ m) and relative intensities (I/I_0/%) of the reflections in the X-ray diffractogram of $NH_4CeTi[Cit(CH_2)_2OH]_3 \cdot HO(CH_2)_2OH \cdot 5.2H_2O$ (main part of the product **6**)[a]

Studied sample		$(NH_4)_2HCitH$[b]		Studied sample		$(NH_4)_2HCitH$[a]	
d	I/I_0[c]	*d*	I/I_0	*d*	I/I_0[b]	*d*	I/I_0
9.68	100			3.210	9		
7.49	9 (19)	7.4	8	3.131	8 (18)	3.133	45
6.93	62			3.033	11 (24)	3.041	65
6.13	24			2.929	10 (22)	2.911	30
6.01	24			2.843	16 (35)	2.848	10
5.75	30 (66)	5.7	60	2.742	6 (13)	2.730	7
5.50	38 (76)	5.4	80	2.677	10 (22)	2.663	20
5.10	10 (22)	5.05	25	2.596	8 (18)	2.589	20
4.85	24			2.510	31	2.520	2
4.36	6 (12)	4.34	7	2.466	3 (5)	2.460	5
3.95	48 (100)	3.92	100	2.232	5 (11)	2.235	8
3.82	48	3.85	2	2.011	6 (13)	2.004	5
3.60	80	3.629	15	1.977	3 (6)	1.964	1
3.272	14			1.866	4 (9)	1.872[d]	2

[a] For symbols meaning see the text
[b] JSPDS 311531
[c] Relative intensities related to the highest reflex of $(NH_4)_2HCitH$ are shown in brackets
[d] For $(NH_4)_3HCit$ according to JSPDS 451540. No data for $(NH_4)_2HCitH$ are reported in this 2θ region

metal ions as monodentate ligand as it is shown in Fig. 5. The shoulder observed near 1575 cm^{-1} might be assigned to a terminal carboxylate group from the bridging ligand (Fig. 5). A similar bonding mode has been proved by IR spectral and X-ray analysis in other citric complexes [16, 17]. The bands in the 1450–1317 cm^{-1} region are caused by the symmetric COO^- stretching vibration. The difference between the wave numbers of the antisymmetric and symmetric stretching vibrations of COO^- confirms [17] the above supposed carboxylate coordination. The vibration of the CH_2 groups (about 1452 cm^{-1}) and the HOH bending of crystallization water molecules (1605 cm^{-1}) may also contribute to the structure of the symmetric and antisymmetric modes. The outline of the COO^- band in the NH_4^+-free product (Fig. 1 (2)) is similar, but not the same. One of the reasons for the observed difference might be the difference between the crystal structure*s* of the crystalline NH_4-containing and X-ray amorphous NH_4-free citrates, confirmed by the X-ray diffractometry.

Part of the water molecules present in the product are bonded stronger, *i.e.* being in the complex's inner sphere they are completing the coordination sphere(s) of the metal(s) (shown by the thermogravimetric analysis; see the next paragraph).

Some of the main characteristics (number of ligands, their average charge, the degree of esterification, the number of ligands with deprotonated alcoholic groups) of the studied complexes containing only one or both metals are compared in Table 5. It is obvious that the latter one could not be a mixture of individual titanium and cerium complexes. If the mixed-metal product was a mixture of the two complexes (in 1:1 molar ratio), the values of the parameters determining its composition should be means of the respective ones of the mononuclear titanium and cerium complexes. The experimental results (Table 5) do not confirm such an assumption; for example, the formal number of ligands in the mixture (1:1) of cerium (**3**) and titanium (**4**) complexes should be $(1.5 + 2.3)/2 = 1.9$ but, actually, it is 3.0. One can see just the same concerning the other parameters which proves that the product containing both Ce and Ti is a complex, qualitatively different from the complexes containing one of the metals only.

The EDAX analysis confirms the constant composition of the NH_4–Ce(IV)–Ti(IV) sample **6**. The mean content of Ce and Ti (relatively to their sum), determined from seven randomly chosen points, is 50.60 and 49.40 mol%. The standard deviations are 0.17 and 0.11% for Ce and Ti, being in the error limits of the method.

The rationalization of the formulae of the complex **5** shown in Table 2 could be done multiplying it by 10. Then the isolated products should be described schematically as a mixture of complexes, one of them with a polynuclear chain-like structure with some

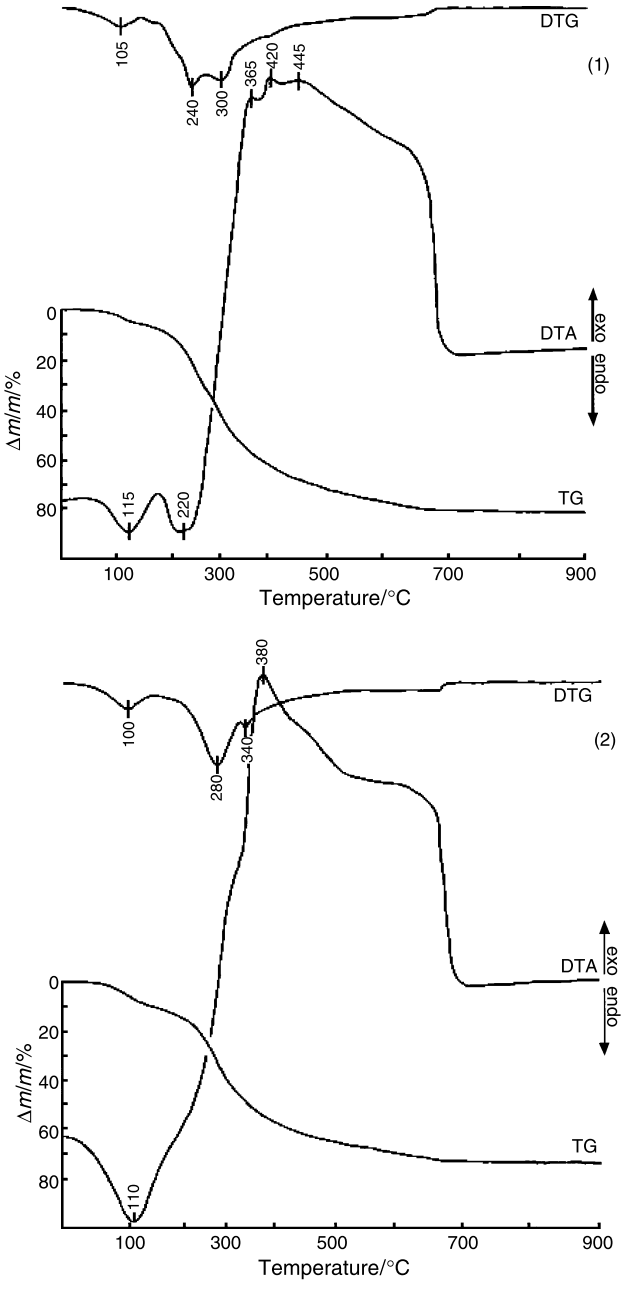

Fig. 7. DTG, DTA, and TG curves of **6** (1) and **5** (2) (see Table 2)

Table 7. Thermal decomposition of the Ce(IV)–Ti(IV) citrates

Sample symbol[a]	Parameters	Stages						
		I		II	III	IV	V	
		a	b				a	b
2	Temperature interval/°C	40–115	115–160			160–180		180–255
	DTG-peak/°C	100						
	DTA-peak[b]/°C	110 (−)						
	$\Delta m/m^c$/% F^c	7.6	3.5			0.9		12.8
	C^c	7.6	3.5			0.9		12.8
	*	$3.9H_2O$	$1.8H_2O$	$0.1H_2O$	–	–	0.1HO*R*OH	2.7*R*O
6	Temperature interval/°C	50–140	140–170	170–200		200–225	225–245	245–275
	DTG-peak/°C	105					240	
	DTA-peak[b]/°C	115 (−)				220 (−)		
	$\Delta m/m^c$/% F^c	6.4	1.9	5.0		5.7	5.4	11.6
	C^c	6.3	1.9	2	2.4	5.7	5.4	11.6
	*	$4H_2O$	$1.2H_2O$	$1.3H_2O$	$1.6NH_3$	0.3*AAE*[d]	HO*R*OH	3*R*O

Sample symbol[a]	Parameters	Stages					
		VI	VII			VIII	Total
			a_1	a_2	b		
2	Temperature interval/°C	255–325		325–375	375–455	455–760	40–760
	DTG-peak/°C		280	340			
	DTA-peak[b]/°C				380 (+)		
	$\Delta m/m^c$/% F^c		21.0	8.1	8.4	10.7	73.0
	C^c		21.1	8.0	8.4	10.5	72.8
	*	$2.7CO_2$	2.7CO	2.7CO	13.4H + 4O	8.1C	
6	Temperature interval/°C	275–305	305–375	375–415	415–490	490–800	50–800
	DTG-peak/°C	300					
	DTA-peak[b]/°C		365 (+)	402 (+)	455 (+)		
	$\Delta m/m^c$/% F^c	13.0	9.8	4.9	6.8	9.5	80.0
	C^c	11.6	9.8	4.9	6.8	9.5	77.9
	*	$3CO_2$	4CO	2CO	14H + 4O	9C	

[a] See Table 2
[b] (−) – endo-, (+) – exo-effect
[c] $\Delta m/m$ – Relative mass loss, *F* experimentally found, *C* calculated according to the proposed scheme (Fig. 8)
[d] $AAE = CH_2COOH–C(COOH)=CHCOO(CH_2)_2OH$
* Separated compounds, mol/mol complex

of the (CitCH$_2$CH$_2$OH^{3-}) species playing the role of bridges {3[CeTi–(CitCH$_2$CH$_2$OH^{3-})$_3$–CeTi–(CitCH$_2$CH$_2$OH^{3-})$_3$–CeTi–(CitCH$_2$CH$_2$OH^{3-})$_2$] · CeTi[Cit(CH$_2$)$_2$OH^{3-}]$_2$[HCit(CH$_2$)$_2$OH^{2-}]} · HO(CH$_2$)$_2$OH · 57H$_2$O (**5**).

The NH$_4$–Ce–Ti-complex **6** is the only one between the studied *Ln*–Ti-citrates with, although poor, crystal structure (Fig. 6). The X-ray pattern shows that the interplanar distances (Table 6) of one of the crystal phases existing in the sample are very close to those of (NH$_4$)$_2$(HCitH). Accounting for the fact that all of the ligands in this product are esterified (Table 2), it has to be accepted that (NH$_4$)$_2$[HCit(CH$_2$)$_2$OH] is present in the system. In such a case the elemental composition of **6** could be described as NH$_4$CeTi[Cit(CH$_2$)$_2$OH^{3-}]$_3$ · HO(CH$_2$)$_2$OH · 5.2H$_2$O · 0.3(NH$_4$)$_2$[HCit(CH$_2$)$_2$OH^{2-}]. The ester groups in (NH$_4$)$_2$[HCit(CH$_2$)$_2$OH] cause an enlargement of most of the interplanar distances compared with the ones in (NH$_4$)$_2$(HCit) by 0.4–0.8%. The other group of reflections (some of them with rather large Full Width at Half of the Magnitude) with interplanar distances ($\times 10^{10}$ m) and their relative intensities (%), namely 9.68 (100), 6.93 (62), 6.13 (24), 6.01 (24), 4.85 (24), 3.82 (44*), 3.60 (47*), 3.272 (14), 3.210 (9), 2.510 (27*) can be assigned to NH$_4$CeTi[Cit(CH$_2$)$_2$OH]$_3$ · HO(CH$_2$)$_2$OH · 5.2H$_2$O. The reflections marked with an asterisk are slightly disturbed by the (NH$_4$)$_2$[HCit(CH$_2$)$_2$OH] reflections and their intensities are corrected accordingly.

Thermal Decomposition of Ce–Ti Complexes

The study of the thermal decomposition of these products also confirms the formulae cited in the previous section. The DTG, TG, and DTA curves are shown in Fig. 7 and corresponding quantitative parameters are summarized in Table 7. The thermochemical behavior of the complexes can be satisfactorily described by the scheme shown in Fig. 8.

It is analogous to the one already proposed in the case of *Ln*(III)–Ti(IV) complexes, which is supported by the identification of most of the intermediates [6, 7]. Nevertheless, some of the scheme details should

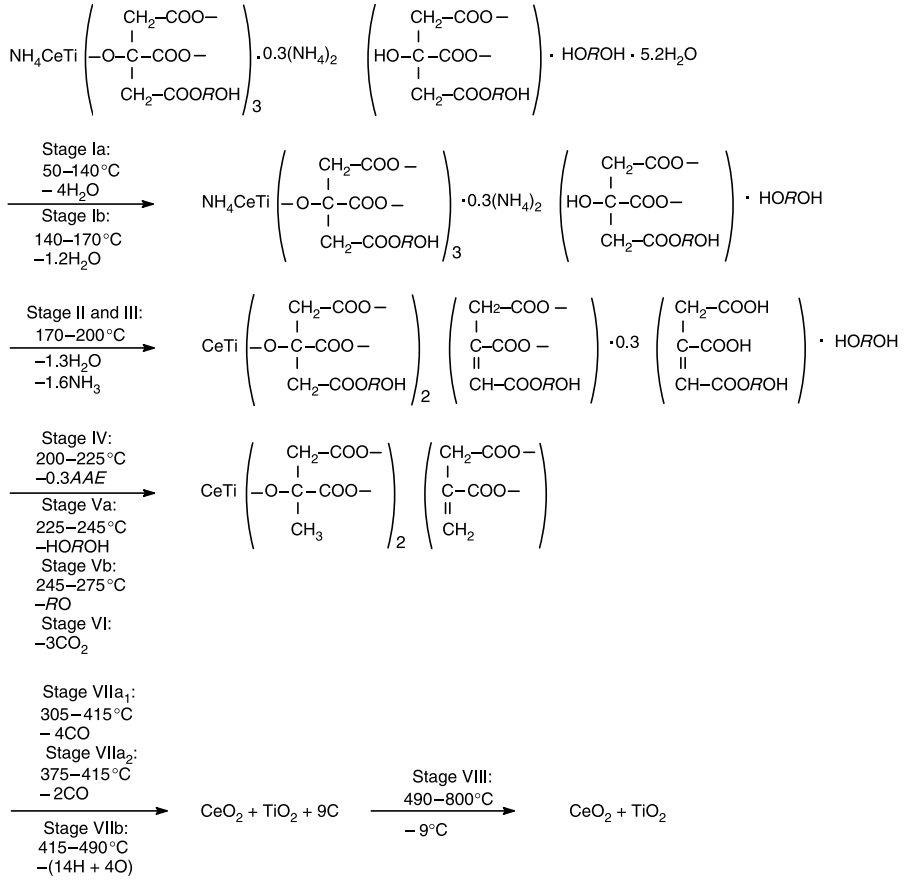

Fig. 8. Thermal decomposition of **6** (see Table 2); $R = (CH_2)_2$, $AAE = CH_2COOHC(COOH)=CHCOOROH$

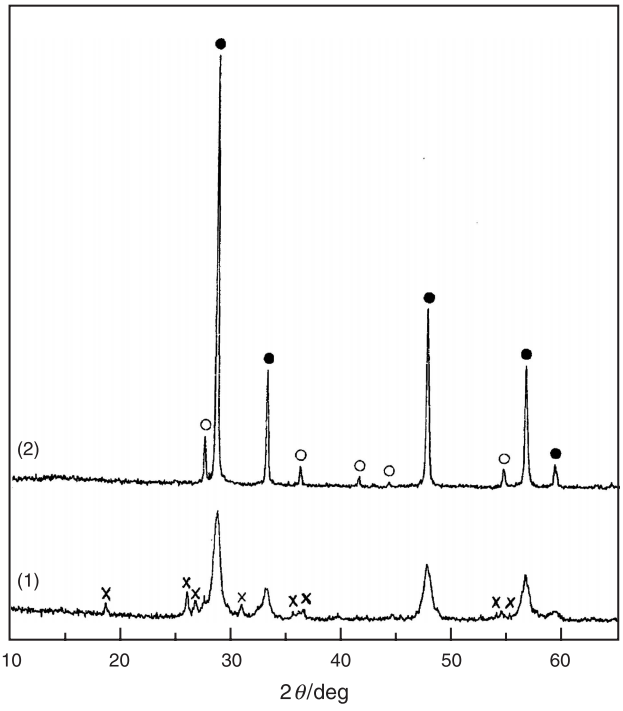

Fig. 9. X-Ray powder diffractograms of the final product of **6** (see Table 2) heated for 4 h at 750°C (1) and at 1000°C (2): • – CeO_2, ○ – TiO_2, X – unidentified phase

be considered as hypothetical ones. The dehydration of the samples proceeds in two steps (stages **Ia** and **Ib** in Fig. 8 and Table 7) and completes at ~170°C. The dehydration continuous as an intramolecular process with the participation of the alcoholic group and hydrogen atoms from the CH_2 group, and the formation of a double C=C bond (**II**). It could be considered that the subsequent release of NH_3 from NH_4^+ (**III**) gives an additional possibility for intramolecular dehydration and, accordingly, the two processes (ammonia release and dehydration) are running simultaneously within the 170–200°C interval. The free aconitic acid ester results from the NH_3 leaving the system at 200–225°C (stage **IV**). Similar behavior is observed earlier [22] in the complex ammonium salts of metal citrates. Up to ~275°C the ethylene glycol is released in two steps: during the first one (**Va**) the ethylene glycol bonded as adduct leaves the system, during the second one a process of deesterification takes place (**Vb**). The decarboxylation of the in such a way formed COOH groups (**VI**) proceeds up to 305°C. In contrast to other analogous lanthanide(III)–titanium(IV) citrates stud-

Table 8. Interplanar distances ($d/10^{-10}$ m) and relative intensities (I/I_0/%) and *Miller* indexes of the reflexes in the X-ray diffractogram of the products obtained after thermal decomposition of NH_4–Ce–Ti-complex **6**

Sample obtained at 750°C		Sample obtained at 1000°C		CeO_2[a]			TiO_2 (rutil)[b]		
d	I/I_0	*d*	I/I_0	*d*	I/I_0	hkl	*d*	I/I_0	hkl
4.7640	12								
3.4432	27								
3.3479	19								
3.2505	20	3.2505	12				3.2500	100	110
3.1184	100	3.1184	100	3.1234	100	111			
2.8956	15								
2.7043	30	2.7043	28	2.7056	30	200			
2.5243	9								
2.4880	10	2.4880	5				2.4870	50	101
2.4617	11								
2.1796	<1	2.1796	2				2.1880	25	111
2.0520	<1	2.0520	<1				2.0540	10	210
1.9118	52	1.9118	42	1.9134	52	220			
1.7017	8								
1.6872	9	1.6872	39				1.6874	60	211
1.6667	8								
1.6320	42	1.6320	29	1.6318	42	311			
1.5595	8	1.5595	8	1.5622	8	222			
1.4503	<1	1.4503	<1				1.4528	10	312

[a] JSPDS No. 34394
[b] JSPDS No. 211276

ied by us, it seems (Fig. 8) that the release of CO from Ce(IV)–Ti(IV) citrates (305–415°C, **VIIa**) proceeds in two steps. The destruction of the organic skeleton is completed up to 490°C (**VIIb**). The residual carbon burns up to 800°C (**VIII**). The X-ray diffraction (Fig. 9, Table 8) indicates CeO_2 and rutil to be the final decomposition products. The experimental mass losses (Table 1) are in satisfactory agreement with the calculated ones according to the proposed scheme.

Ln(III)- and Ce(IV)-Titanium Complexes – A Comparison

In search for the factors determining the composition of the complexes formed in the course of PCM application, studying the La(III)–Ti(IV) and Y(III)–Ti(IV) citrates, it was shown [3, 5] that some competing processes take place during the formation of the complexes: adduct formation, esterification and complexation through deprotonated COOH and OH groups. When the synthesis of Ln(III)–Ti(IV) citrates is performed at low temperature (40°C) the esterification degree of the ligands is relatively low (*i.e.* the COO^- groups are available for coordination) and OH deprotonation is insignificant. The increase of the temperature favored the esterification and provoked the OH deprotonation as a way for a compensation of the COO^- insufficiency. One could suppose that, substituting Ln(III) as a complexing agent for Ce(IV), the COO^- insufficiency will be increased thus giving rise to OH deprotonation. That is why it was of special interest to compare the analogous La(III)–Ti(IV) and Ce(IV)–Ti(IV) citrates. Some of the main features of both complexes' composition are juxtaposed in Table 5. As it was expected, the most significant difference is in the relative content of ligands with deprotonated alcoholic groups.

The increase of the charge (the oxidation state) of the complexing agent, when La(III) or Y(III) is substituted for Ce(IV), can not be compensated by the increase of the ligands number – it seems that the steric hindrance limits this number to three. The compensation might be realized by a decrease of the esterification degree or/and by an increase of the number of deprotonated OH groups. The experimental data (Table 5) show that the competition between the esterification and the complexation causes the realization of both effects in the Ce(IV)–Ti(IV) complex, namely, the esterification degree decreases (in comparison with the La analogue) by $\sim 1/3$ and, at the same time, the alcoholic group of all of the ligands is being deprotonated.

Experimental

The $Ce(NO_3)_3 \cdot 6H_2O$, $(NH_4)_2Ce(NO_3)_6$, anhydrous citric acid, ethylene glycol, $Ti[OCH(CH_3)_2]_4$, and acetone, all of them of p.a. grade, were used as received in the synthesis and isolation of the complexes.

The complexes preparation method described earlier [5] was used at molar ratios Ce^{3+}:citric acid:ethylene glycol = 1:4.3:17.1; Ti^{4+}:citric acid:ethylene glycol = 1:5.7:22.8, and Ce^{n+}:Ti^{4+}:citric acid:ethylene glycol = 1:1:10:40. The solutions obtained were heated with stirring for 0.5 h at 100°C. A longer heating time (1 h) was applied when synthesis was performed at 40°C to ensure the satisfactory processing of the complexation. Above 100°C the reaction turned to be strongly exothermic and viscosity of the solutions sharply increased. After cooling down to room temperature acetone was added in a volume of 10 times larger than the volume of the mother liquid. Further increase of the added acetone quantity did not lead to the complexes' yield increase. After 24 h the formed precipitates were separated, soaked in fresh acetone for additional 24 h, filtered off, washed with plenty of acetone, and dried in air.

The contents of H, C, and N were determined by the common organic analysis method. The determination of Ce and Ti was performed by Inductively Coupled Plasma Atomic Emission Spectroscopy (ICP-AES) in solution, obtained by melting $\sim$0.5 g of the sample with $\sim$10 g $KHSO_4$ and dissolving the melt in H_2SO_4 (5%). The lines of Ti at 323.66 nm and Ce at 413.38 nm were singled out for ICP-AES analysis according to Ref. [23, 24]. The content of cerium in Ti-free products was confirmed by cerimetric analysis; solutions were prepared by dissolving the residues in 65% HNO_3 after heating the samples at 600°C. The IR spectra (4000–400 cm^{-1}) were recorded by a Bomem Michelson 100 FTIR or Specord 75 (Carl Zeiss) spectrometers; KBr pellets or nujol mulls were used. The ^1H and ^{13}C NMR spectra of complexes in D_2O solution were taken using a Bruker 250 MHz spectrometer. The ^{13}C cross polarization (CP) magic angle spinning (MAS) spectra of the solids were recorded on a Bruker MSL-300 instrument at 75.5 MHz, the samples were spun at 8.4 kHz in a 4 mm ZrO_2 rotor. The DTA, DTG, and TG curves were recorded by a Paulik-Paulik-Erdey (MOM, Hungary) derivatograph. The samples were heated (10°C/min) in static air in a synthetic corundum crucible. Energy dispersive X-ray microanalysis was performed by means of a JOEL Superprobe-733 instrument (Japan) with 25 kV accelerating voltage. The X-ray powder diffractograms of the complexes were taken by a Siemens powder diffractometer using CoKα radiation at 40 kV and 40 mA with a scan rate of 0.3°/min and the diffraction pattern of the residues after ignition was taken by a TUR-M62 (Germany) diffractometer using CuKα radiation at 30 kV and 20 mA with a scan rate of 0.9°/min.

The *ab initio* calculations were carried out using GAUSSIAN 03 [25] quantum chemistry program package. The structure

optimization of the Ti^{4+}–Ce^{4+} citric complex was performed at the restricted *Hartree-Fock* (*RHF*) level without any symmetry constrains (C_1 symmetry was assumed). The calculations were carried out with the *Stewens-Basch-Krauss-Jasien* effective core potentials (ECP) and their concomitant basis sets for all the atoms (ECP-31G) [26–28].

Acknowledgement

The study was supported partially by the Bulgarian National Science Fund under Contract X-504.

References

[1] Milanova MM, Kakihana M, Arima M, Yashima M, Yoshimura M (1996) J Alloys Comp **224**: 6
[2] Kakihana M, Milanova MM, Arima M, Okubo T, Yashima M, Yoshmura M (1996) J Am Ceram Soc **79**: 1673
[3] Milanova MM, Arnaudov MG, Getsova MM, Todorovsky DS (1997) J Alloys Comp **264**: 95
[4] Arnaudov MG, Getsova MG, Todorovsky DS, Milanova MM (1998) Anal Lab **7**: 70
[5] Getsova MM, Todorovsky DS, Arnaudov MG (2000) Z Anorg Allg Chemie **626**: 1488
[6] Todorovsky DS, Getsova MM, Vasileva MA (2002) J Mat Sci **37**: 4029
[7] Getsova M, Todorovsky D (2000) Bulg Chem Commun **32**: 89
[8] Arima M, Kakihana M, Nakamura Y, Yashima M, Yoshimura M (1996) J Am Ceram Soc **79**: 2847
[9] Kakihana M, Okubo T, Arima M, Uchiama O, Yashima M, Yoshimura M, Nakamura Y (1997) Chem Mat **9**: 451
[10] Zhou Z-H, Deng Y-F, Jiang JQ, Wan H-L, Ng S-W (2006) Dalton Trans 2636
[11] Kefalas ET, Panagiotidis P, Raptopoulou CP, Terzis A, Mavromoustakos T, Salifoglou A (2005) Inorg Chem **44**: 2596
[12] Collins JM, Uppal R, Incarvito CD, Valentine AM (2005) Inorg Chem **44**: 4331
[13] Todorovsky D, Petrova N, Getsova M, Todorovska R, Manolov I, Groudeva-Zotova S (2004) Key Eng Mat **264–268**: 359
[14] Glusker JP, Minkin JA, Patterson AL (1969) Acta Cryst **B25**: 1066
[15] Roelofsen G, Cauters JA (1972) Cryst Struct Commun **1**: 23
[16] Fujita T (1982) Chem Pharm Bull **30**: 3461
[17] Nakamoto K (1977) Infrared and Raman Spectra of Inorganic and Coordination Compounds, Wiley, New York, p 59
[18] Cudby ME (1988) Ekt Spectr News **78**: 18
[19] Breitmeier E, Voelter W (1987) Carbon-13 NMR Spectroscopy, VCH, Weinheim, p 226
[20] Strouse J, Layten SW, Strouse CE (1977) J Am Chem Soc **99**: 562
[21] Todorovsky D, Getsova M, Wawer I, Stefanov P, Enchev V (2004) Mater Lett **58**: 3559
[22] Zhecheva E, Stoyanova R, Gorova M, Alcantara R, Morales J, Tirado JL (1996) Chem Mater **8**: 1429
[23] Daskalova N, Velichkov S, Slavova P, Ivanova E (1997) Spectrochim Acta **B52**: 257
[24] Daskalova N, Velichkov S, Krasnobaeva N, Slavova P (1992) Spectrochim Acta **B47**: E1595
[25] Frisch MJ, Trucks GW, Schlegel HB, Scuseria GE, Robb MA, Cheeseman JR, Montgomery Jr JA, Vreven T, Kudin KN, Burant JC, Millam JM, Iyengar SS, Tomasi J, Barone V, Mennucci B, Cossi M, Scalmani G, Rega N, Petersson GA, Nakatsuji H, Hada M, Ehara M, Toyota K, Fukuda R, Hasegawa J, Ishida M, Nakajima T, Honda Y, Kitao O, Nakai H, Klene M, Li X, Knox J, Hratchian HP, Cross JB, Adamo C, Jaramillo J, Gomperts R, Stratmann RE, Yazyev O, Austin AJ, Cammi R, Pomelli C, Ochterski JW, Ayala PY, Morokuma K, Voth GA, Salvador P, Dannenberg JJ, Zakrzewski VG, Dapprich S, Daniels AD, Strain MC, Farkas O, Malick DK, Rabuck AD, Raghavachari K, Foresman JB, Ortiz JV, Cui Q, Baboul AG, Clifford S, Cioslowski J, Stefanov BB, Liu G, Liashenko A, Piskorz P, Komaromi I, Martin RL, Fox DJ, Keith T, Al-Laham MA, Peng CY, Nanayakkara A, Challacombe M, Gill PMW, Johnson B, Chen W, Wong MW, Gonzalez C, Pople JA (2003) Gaussian Inc., Pittsburgh PA
[26] Stevans W, Basch H, Krauss J (1984) J Chem Phys **81**: 6028
[27] Stevans W, Basch H, Krauss J (1992) Ca J Chem **81**: 612
[28] Cundari TR, Stevans WJ (1993) J Chem Phys **98**: 5555